PDRS AND SHOCKS IN S106 IR AND CEP A EAST

M.E. VAN DEN ANCKER
Astronomical Institute, University of Amsterdam

P.R. WESSELIUS
SRON Groningen

A.G.G.M. TIELENS
NASA Ames Research Center

AND

L.B.F.M. WATERS
Astronomical Institute, University of Amsterdam

Abstract. We present SWS grating scans of pure H_2 rotational lines, as well as several infrared fine-structure lines for two embedded Young Stellar Objects, S106 IR and Cep A East. Excitation temperatures and masses were derived from the low-lying pure rotational levels of H_2 and are 490 and 740 K and 0.04 and 0.007 $M_\odot$ for S106 and Cep A, respectively. The observations were compared to theoretical models for PDRs and dissociative and non-dissociative shocks. The infrared spectrum of S106 IR is dominated by PDR emission while that of Cep A East has a large shock component. We suggest that the difference between these two objects could reflect an evolutionary trend.

1. Introduction

The infrared emission-line spectrum of Young Stellar Objects (YSOs) is dominated by the interaction of the central object with the remnants of the cloud from which it formed. The intense UV radiation from accretion as well as from the central star itself causes destruction of dust and molecular material close to the YSO and ionizes much of the atomic material, giving rise to typical nebular lines. The strong stellar wind, often collimated into a bipolar outflow, will cause a shock wave as it penetrates in the surrounding molecular cloud, warming the post-shock gas to sufficient temperatures

TABLE 1. Observed and extinction-corrected line fluxes (in 10^{-14} W m^{-2}).

Line	λ	S106 IR		Cep A East	
	[μm]	Obs.	Ext. corr.	Obs.	Ext. Corr.
H_2 0–0 S(0)	28.2188	–	–	–	–
H_2 0–0 S(1)	17.0348	0.81	1.30	0.09	0.20
H_2 0–0 S(2)	12.2786	–	–	–	–
H_2 0–0 S(3)	9.6649	0.33	1.25	0.10	0.92
H_2 0–0 S(4)	8.0251	0.19	0.30	0.17	0.36
H_2 0–0 S(5)	6.9095	0.21	0.27	0.31	0.47
H_2 0–0 S(6)	6.1086	–	–	0.09	0.15
H_2 0–0 S(7)	5.5112	–	–	0.21	0.36
H_2 0–0 S(8)	5.0531	–	–	0.05	0.09
H_2 0–0 S(9)	4.6946	–	–	0.08	0.16
H_2 0–0 S(10)	4.4099	–	–	0.06	0.13
H_2 0–0 S(11)	4.1813	–	–	–	–
[Fe I] ($^5D_4$–$^5D_3$)	24.0423	–	–	–	–
[Fe I] ($^5D_3$–$^5D_2$)	34.7133	–	–	–	–
[Fe II] ($^4F_{9/2}$–$^4F_{7/2}$)	17.9410	0.15	0.25	0.05	0.12
[Fe II] ($^6D_{9/2}$–$^6D_{7/2}$)	25.9882	3.27	4.35	0.11	0.18
[Fe II] ($^6D_{7/2}$–$^6D_{5/2}$)	35.3491	1.26	1.50	0.24	0.32
[S I] ($^3P_2$–$^3P_1$)	25.2490	–	–	0.41	0.68
[Si II] ($^2P_{1/2}$–$^2P_{3/2}$)	34.8140	16.7	20.0	0.51	0.69

to cause strong molecular and ionic emission. Here we will present new ISO SWS data on the infrared fine-structure lines and molecular hydrogen emission from two such YSOs: the central region of the bipolar nebula S106, and the eastern part of the complex molecular outflow source Cep A.

Neutral clouds irradiated by far-ultraviolet photons are known as photodissociation regions (PDRs). In these regions, heating of the gas occurs by collisions of photoelectrically ejected electrons from grain surfaces. Cooling of the gas occurs mainly through emission in atomic fine-structure and molecular lines, reaching observable intensities in a wide range of astronomical objects.

In shock waves the molecular gas is heated by compression of a supersonic wave moving into teh gas (e.g. Draine & McKee 1993). Shocks are usually divided into two types. In J- or Jump-shocks viscous heating of the neutrals occurs in a thin shock front in which radiative cooling is insignificant, and the post-shock gas is heated to several times 10^4 degrees, dissociating all molecular material. Cooling of the post-shock gas occurs trough atomic fine-structure lines in the shock as well as through re-formation of molecules in the post-shock gas. C- or Continuous-shocks are magnetized,

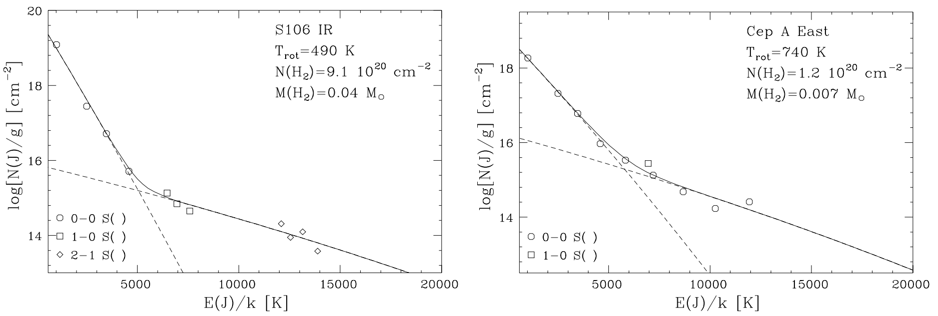

Figure 1. H_2 excitation diagram for S106 (left) and Cep A East (right). ISO observations of pure rotational lines are indicated by the circles. Diamonds and squares indicate ground-based measurements of ro-vibrational lines from literature. The dotted lines show the Boltzmann distribution fits to the low-lying pure rotational lines and all lines with upper level energies above 5000 K. The solid line indicates the sum of both contributions

non-dissociative shocks in which a trace fraction of ions and the magnetic field are compressed ahead of the shock front and are able to heat the neutral gas to a few thousand degrees. Cooling occurs mainly through radiation from molecular material. If the temperatures in a C-shock become sufficiently high to start to dissociate molecules, the cooling through the molecular lines goes down, and the shock temperature increases until it turns into a J-shock. Shocks with a shock velocity larger than 40 km s^{-1} are usually J-shocks, while slower shocks are usually of C-type.

2. Observations

ISO Short Wavelength Spectrometer (SWS) grating scans (AOT 2) of selected molecular and fine transition lines of S106 IR and Cep A East were obtained in ISO revolutions 134 and 220, respectively. Data were reduced in a similar fashion as done by the automated pipeline, but with manual checks of the level of dark currents. Scanned lines and measured line fluxes for detected lines are listed in Table 1. Errors in these fluxes are expected to be smaller than 30%. Probably the H_2 0–0 S(2) line escaped detection because of fringing problems in this part of the spectrum.

3. Molecular Hydrogen emission

From the H_2 line fluxes we calculated the apparent column densities in the upper J levels, N(J), after correcting for extinction using values of A_V of 24 and 40^{m} for S106 IR and Cep A East, respectively (Eiroa et al. 1979; Felli et al. 1984). This correction is especially important for the 0–0 S(3) line at 9.66 μm, since it is affected by the silicate absorption feature in the

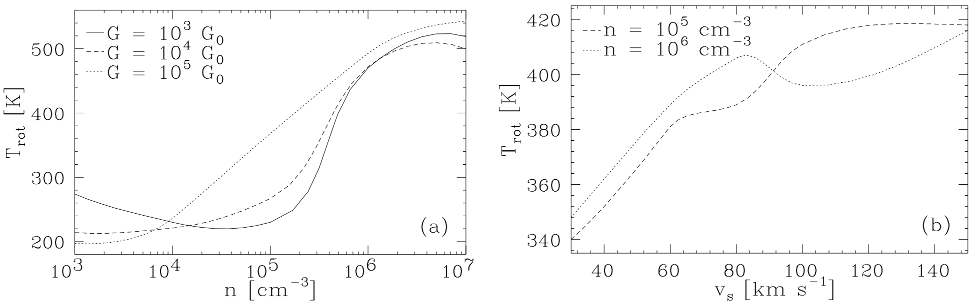

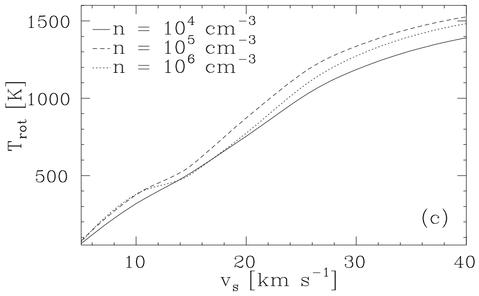

Figure 2. Theoretical relation between a) $T_{\rm rot}$ and n for PDR models, b) $T_{\rm rot}$ and v_s for J-shock models, and c) $T_{\rm rot}$ and v_s for C-shock models

extinction curve.

In Fig. 1 we plot $\log N(\mathrm{J})/g$ versus the energy of the upper level, assuming the high temperature equilibrium relative abundances of 3:1 for the ortho and para forms of H_2 (Burton et al. 1992). For a Boltzmann distribution, the slope of the points in such a plot is inversely proportional to the excitation temperature and the intercept is a measure of the column density of warm gas. A fit of a Boltzmann distribution to the low lying lines results in values of 490 K and 9×10^{20} cm^{-2} and 740 K and 1×10^{20} cm^{-2} for S106 IR and Cep A East. With the distances to S106 and Cep A of 600 and 690 pc, this corresponds to H_2 masses of 0.04 and 0.007 $M_\odot$.

Also plotted in Fig. 1 are several measurements of H_2 ro-vibrational lines in S106 and Cep A from literature. In the case of S106, the relative location of the 1–0 and 2–1 S(1)-lines in Fig. 1 are indicative of fluorescent excitation through UV pumping (Black & van Dishoeck 1987; Draine & Bertoldi 1996). In the case of Cep A, these lines may indicate the presence of a smaller column (10^{18} cm^{-2}) of hot (a few 1000 K) molecular hydrogen, in addition to the larger column of warm gas.

Using PDR, J-shock and C-shock model predictions by Burton et al. (1992), Hollenbach & McKee (1989) and Kaufman & Neufeld (1996), we determined the excitation temperature $T_{\rm rot}$ from the H_2 low-lying pure rotational levels from these models as a function of density n and either incident FUV flux G (in units of the average interstellar FUV field G_0) or shock velocity v_s in an identical way as was done for the observations. The resulting relations between $T_{\rm rot}$ and n or v_s are shown in Fig. 2. The PDR and J-shock models predict a fairly small (200–540 K) range of resulting excitation temperatures, whereas in the C-shocks this range is much larger (100–1500 K). Furthermore, we see that in the model predictions for shocks the resulting $T_{\rm rot}$ does not depend much on density, whereas for PDRs it does not depend much on G, suggesting that once the mechanism of the H_2 emission is established, it can be used to constrain v_s or n.

Comparing the excitation temperatures of 490 and 740 K for S106 and Cep A with those plotted in Fig. 2, we note that for S106 this falls well within the range of PDR- and C-shock model predictions, but are too high compared to the ones expected from J-shocks. The observed bright PAH emission features and the atomic fine-structure line spectrum (§4) point towards a PDR origin for the H_2 emission in S106. The higher temperature for Cep A can only be reproduced by the C-shock models. Therefore we tentatively conclude that a dense ($\geq 10^6$ cm^{-3}) PDR seems to be the best candidate to explain the observed H_2 emission in S106 IR and a slow ($\approx$ 20 km s^{-1}) non-dissociative shock can explain the observed warm column of H_2 in Cep A East. Given that the regions we are looking at probably only fill part of the SWS beam, the absolute intensity of the H_2 emission listed in Table 1 can also be reproduced by these same models.

4. Fine Structure Lines

Important constraints on the possible excitation mechanisms come from the observed fine structure lines. The observed surface brightness for the [Si II] line in S106 requires a density higher than $\approx 10^5$ cm^{-3} and $G \geq 10^5$ G$_0$ in the Tielens & Hollenbach (1985) PDR models. This regime can also reproduce the observed ratios of [Si II] and the [Fe II] lines. The predicted intensities of [S I] and [Fe I] are sufficiently low to be undetectable, in agreement with the observations. We conclude that S106 contains a PDR.

For Cep A the situation is more complicated. From the detection of the [S I] line at 25.25 μm, we know that either a J- or C-shock must be present. From the detection of [Si II] and [Fe II] emission we know that either a J-shock or PDR must be present as well (C shocks can only contain trace fractions of ions). We have used J-shock models to fit the fine structure lines. Due to aperture size effects we only attempt to fit the line strength ratios in identical SWS apertures. To reproduce both the ratio of [Fe II] 26.0 μm to [S I] 25.2 μm and the ratio of [Fe II] 35.3 μm to [Si II] 34.8 μm as well as fit the [Fe I] upper limit, the Hollenbach & McKee (1989) J-shock models require a high (10^6 cm^{-3}) density with a moderately fast ($\approx$ 60 km s^{-1}) shock. The predicted surface brightnesses are higher than those observed, in agreement with a shock only filling part of the SWS beam.

5. Discussion and Conclusions

One or multiple J-shocks cannot reproduce the observed H_2 emission in Cep A East. The success of the J-shock model in explaining the observed fine-structure lines and the absence of PAH emission, excluding the possibility of a significant contribution from a PDR, leads us to pose that a combination of one or more J- and C-shocks must be present in Cep A. In this picture, the [Si II] and [Fe II] emission would originate completely in the J-shock, whereas both the C- and the J-shock would contribute to the observed [S I] and H_2 spectra. The observed hot column of H_2 in Cep A may then be due to formation pumping (the effect that H_2 gets re-formed with non-zero energy in the post-shock gas) in the J-shock. The presence of more than one type of shock could be linked to the reported multiple episodes of outflow activity from the embedded source (Narayanan & Walker 1996). Alternatively, the stellar wind material could be slowed down by a (fast) J-shock while the surrounding molecular cloud might be swept up by a slower C-shock.

We have shown that in the case of S106 IR we can reproduce the observed infrared H_2 emission and fine structure lines as arising in a PDR with $n \approx 10^6$ cm^{-3} and $G \approx 10^5$ G$_0$. For Cep A we needed both a C- and J-type shock, with shock velocities of about 20 and 60 km s^{-1} respectively, and densities of $\approx 10^6$ cm^{-3} to explain the infrared line-spectrum. The observed H_2 mass in both S106 and Cep A is only a few hundredths of M$_\odot$, whereas several solar masses of H_2 are expected to be present in these star forming regions. This implies that the bulk of the molecular hydrogen must be much cooler than that observed here.

The differences between the environment of these two massive embedded YSOs, S106 and Cep A, are remarkable; In S106 the stellar wind and UV radiation of the exciting source have cleared and excited a sufficiently large region to create strong PDR emission, whereas in the case of Cep A, the central source is still heavily embedded and we observe the interaction of its outflow with its surroundings. Possibly this difference between these two sources is a reflection of their different evolutionary status.

Acknowledgements. LBFMW acknowledges financial support through an NWO *Pionier* grant.

References

Black, F.H., van Dishoeck. E.F. 1987, ApJ 322, 412
Burton, M.G., Hollenbach, D.J., Tielens, A.G.G.M. 1992, ApJ 399, 563
Draine, B.T., Bertoldi, F. 1996, ApJ 468, 269
Draine, B.T., McKee, C.F. 1993, Ann. Rev. A&A 31, 373
Eiroa, C., Elsässer, H., Lahulla, J.F. 1979, A&A 74, 89
Felli, M., Staude, H.J., Reddmann, T., Massi, M., Eiroa, C. et al. 1984, A&A 135, 261
Hollenbach, D.J., McKee, C.F. 1989, ApJ 342, 306
Kaufman, M.J., Neufeld, D.A. 1996, ApJ 456, 611
Narayanan, G., Walker, C.F. 1996, ApJ 466, 844

Tielens, A.G.G.M., Hollenbach, D.J. 1985, ApJ 291, 722